Study of CO_2 Adsorption Time for Carbonate Species and Linear CO_2 Formations onto Bimetallic CaO/Fe_2O_3 by Infrared Spectroscopy

(Kajian Masa Penjerapan CO_2 untuk Pembentukan Spesies Karbonat dan CO_2 Linear pada Dwilogam CaO/Fe_2O_3 oleh Spektroskopi Inframerah)

AZIZUL HAKIM LAHURI* & MOHD AMBAR YARMO

ABSTRACT

The CO_2 adsorption time for carbonate species and linear CO_2 formation onto bimetallic CaO/Fe_2O_3 was investigated. The total basicity for CaO/Fe_2O_3 was 52.85 cm^3g^{-1} which is located at a medium basic site with maximum CO desorption temperature at 454 °C. The CO_2 adsorption was conducted by using a fluidized bed reactor at 4, 12, 24 and 36 h. The element distribution on the adsorbent showed carbonate formation through an increment of the C element when the CO_2 adsorption time was longer. At 4 h of CO_2 adsorption, the adsorbent is capable of generating bicarbonate, monodentate carbonate and bidentate carbonate species. The vibrational modes of the physisorbed linear CO_2 for CO_2 absorbed product at the absorption region of 2240-2402 cm^{-1} was identified after 36 h of CO_2 adsorption. The absorption bands were assigned according to the adjacent CO_2 molecule interactions giving formation of the core layer and second layer linear CO_2 on the CaO/Fe_2O_3 surfaces. The results of the present work show that the addition of CaO on the Fe_2O_3 surfaces enhanced the basic site of the adsorbent which could generate several carbonate species and CO_2 adsorbed products at ambient condition.

Keywords: Bimetallic; calcium oxide; carbonate formation; CO_2 capture; iron(III) oxide

ABSTRAK

Masa penjerapan CO_2 bagi pembentukan karbonat dan CO_2 linear di atas dwilogam CaO/Fe_2O_3 telah dikaji. Jumlah kebesan bagi CaO/Fe_2O_3 adalah sebanyak 52.85 cm^3g^{-1} terletak di tapak bes medium dengan suhu penyahjerapan CO maksimum pada 454 °C. Penjerapan CO_2 dilakukan dengan menggunakan reaktor lapisan terbendalir selama 4, 12, 24 dan 36 jam. Taburan unsur pada penjerap telah menunjukkan bukti pembentukan karbonat melalui peningkatan bagi unsur C apabila masa penjerapan CO_2 semakin lama. Selepas penjerapan CO_2 selama 4 jam, penjerap berkeupayaan dalam menghasilkan spesies bikarbonat, karbonat monodentat dan karbonat bidentat. Mod getaran bagi CO_2 linear yang terjerap secara fizikal untuk hasil CO_2 terjerap pada bahagian serapan 2240-2402 cm^{-1} adalah jelas dikenal pasti setelah 36 jam penjerapan CO_2. Jalur serapan ditentukan berdasarkan interaksi molekul CO_2 berdekatan yang memberikan pembentukan lapisan teras dan lapisan kedua CO_2 linear pada permukaan CaO/Fe_2O_3. Hasil kajian ini menunjukkan penambahan CaO pada permukaan Fe_2O_3 telah memperbaiki tapak bes bagi penjerap yang membolehkan pembentukan spesies karbonat dan CO_2 linear pada keadaan ambien.

Kata kunci: Dwilogam; ferum(III) oksida; kalsium oksida; pembentukan karbonat; penjerapan CO_2
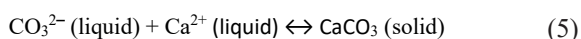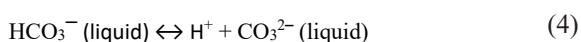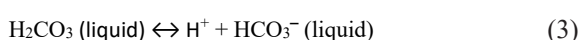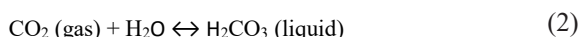
INTRODUCTION

A relatively large amount of mineral groups in the earth's crust is carbonate. The common carbonate minerals are calcite, aragonite (calcium carbonate, $Ca(CO_3)$) which exhibits different crystal system of hexagonal and orthorhombic respectively; magnesite (magnesium carbonate, $Mg(CO_3)$); dolomite ($CaMg(CO_3)_2$); ankerite ($CaMg(CO_3)_2$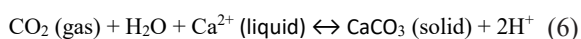); and siderite ($Fe(CO_3)$). Carbonate formation through natural sequestration of carbon dioxide (CO_2) by adsorption/absorption from the atmosphere at the terrestrial and sea as a reservoir. The complex interactions were involved in the natural sequestration by the capability of terrestrial and sea. Around a third of the CO_2 emitted by fossil fuel burning was absorbed

naturally by the seawater (Barker & Ridgwell 2012). The CO_2 equilibrium reaction started by dissolving gaseous CO_2 into liquid CO_2 (1) and forming carbonic acid, H_2CO_3 (2). Carbonic acid rapidly dissociates to produce bicarbonate ions, HCO_3^- (3), wherein the HCO_3^- ions also could dissociate into carbonate ions, CO_3^{2-} (4). Finally, the CO_3^{2-} ions are adsorbed and captured by Ca^{2+} ions in the sea (5) to give calcium carbonate, $CaCO_3$. The overall equation of the CO_2 equilibrium reaction series is shown in Equation 6 produces $CaCO_3$ and H^+ ions.

Half equation:

$$CO_2 \text{ (gas)} \leftrightarrow CO_2 \text{ (liquid)} \tag{1}$$

$$CO_2 \text{ (gas)} + H_2O \leftrightarrow H_2CO_3 \text{ (liquid)} \tag{2}$$

$$H_2CO_3 \text{ (liquid)} \leftrightarrow H^+ + HCO_3^- \text{ (liquid)} \tag{3}$$

$$HCO_3^- \text{ (liquid)} \leftrightarrow H^+ + CO_3^{2-} \text{ (liquid)} \tag{4}$$

$$CO_3^{2-} \text{ (liquid)} + Ca^{2+} \text{ (liquid)} \leftrightarrow CaCO_3 \text{ (solid)} \tag{5}$$

Overall equation:

$$CO_2 \text{ (gas)} + H_2O + Ca^{2+} \text{ (liquid)} \leftrightarrow CaCO_3 \text{ (solid)} + 2H^+ \tag{6}$$

The absorption of CO_2 into seawater increases buffer capacity and reduces CO_2 level in the atmosphere (Hare et al. 2020). Therefore, the natural CO_2 equilibrium is the idea of CO_2 capture which is beneficial to mitigate the rising of anthropogenic CO_2 level in the atmosphere.

The most mature CO_2 capture technology by amine scrubbing has been investigated to separate CO_2 from natural gas since 1930 (Bottoms 1930). Many amine solvents were tested for the CO_2 adsorption capacity but the monoethanolamine (MEA) undoubtedly is the most extended solvent (Luis 2016). Nonetheless, MEA is also corrosive when used at higher concentrations (Bui et al. 2018), whereas ammonia and other amine-based solvents showed disadvantages of high volatility, extensive energy penalty and sensitivity to impurities (Yuan & Eden 2016). It was extended to explore the CO_2 capture activity by developing physical and chemical absorption of amine-based supported materials (Abu Tahari et al. 2020, 2017a, 2017b, 2016, 2015a, 2015b), but the amine molecules tend to block the support materials causing low in adsorption quantity and amine molecule thermally degeneration (Yuan & Eden 2016). These drawbacks are the challenges for researchers to expand the CO_2 capture by the solid sorbent.

An acidic CO_2 molecule has a strong affinity towards solid sorbent surfaces due to the adsorption process that trapping and/or binding the CO_2 molecules to the surface. The nature of the interaction is classified into physical adsorption and chemical adsorption. Physical adsorption involves physisorbed CO_2 by physical forces such as Van der Waals, dipole-dipole, apolar, electrostatic or hydrophobic association, Ho et al. (2014) which exhibiting the mean free energy below 8 $kJmol^{-1}$, Lahuri et al. (2020a) and bond energy is 8-41 $kcalmol^{-1}$. Meanwhile, chemical adsorption is chemisorbed CO_2 that associated with the covalent, chemical bond, ionic or metallic, where the mean free energy for chemical adsorption 8-16 kJ/mol, strong chemical adsorption is above 16 $kJmol^{-1}$ and bond energy is about 60-418 $kcalmol^{-1}$ (Ho et al. 2014).

CO_2 capture through adsorption process was explored onto classical basic metal oxide adsorbent of CaO (Abanades 2002; Barker 1973; Salvador et al. 2003; Silaban & Harrison 1995). Other main group metal oxides were also reported such as MgO (Bhagiyalakshmi et al. 2010; Heo & Park 2017; Kumar et al. 2015; Whateley 1971), SrO (Bagherisereshki et al. 2018), γ-$Al(OH)_3$ (Su & Suarez 1997). There were several attempts by researchers using transition metal oxides such as AgO (Okawa & Tanaka 1995), TiO_2 (Takahashi et al. 2002), ZrO_2 (Yoshikawa et al. 2014), iron oxides (FeO, Fe_2O_3, Fe_3O_4) (Hakim et al. 2016a, 2016b, 2016c, 2015a; Ismail et al. 1997), NiO (Hakim et al. 2015b), CuO (Wan Isahak et al. 2015), Bi_2O_3 (Lahuri et al. 2020a), ZnO (Lahuri et al. 2020b; Wang et al. 2007), Co_3O_4 (Lahuri et al. 2020b). Meanwhile, the CO_2 adsorption capability onto rare earth metal oxides such as La_2O_3 (Bakiz et al. 2010; Horiuchi et al. 1998; Rosynek & Magnuson 1977), $La(OH)_3$ (Rosynek & Magnuson 1977), CeO_2 (Lahuri et al. 2020b; Slostowski et al. 2017; Yoshikawa et al. 2014), CeO_4, Pr_2O_3, and Nd_2O_3 (Horiuchi et al. 1998) were also reported.

While the formation of carbonate species (bicarbonate, monodentate carbonate, bidentate carbonate, and polydentate carbonate) and CO_2 adsorbed product on the single metal oxides/hydroxides such as iron oxides (FeO, Fe_2O_3, Fe_3O_4) (Hakim et al. 2016a), MgO (Whateley 1971), CeO_2 (Yoshikawa et al. 2014), La_2O_3, $La(OH)_3$ (Rosynek & Magnuson 1977), γ-$Al(OH)_3$, and α-FeOOH (Su & Suarex 1997), were reported using infrared spectroscopy. CO_2 adsorbed product that possesses physisorbed linear CO_2 was also reported (Galhotra 2010; Yang & Woll 2017). Although bimetallic metal oxide system such as CaO/CuO (Manovic et al. 2011), Cu/Ni nanoparticles (Austin et al.

2016), $CaO-Al_2O_3$, $CaO-Y_2O_3$ (Naeem et al. 2017), BeO/Fe_2O_3 (Lahuri et al. 2020c) were studied its CO_2 capture efficacy, these works were not extended to the phenomena formation of carbonate and CO_2 adsorbed product on bimetallic system. Among iron oxides, Fe_2O_3 was found to be the most promising adsorbent for CO_2 capture (Hakim et al. 2016a). This work shows the extended work of the bimetallic system CaO/Fe_2O_3 (Lahuri et al. 2017) for the trend of carbonate formation and CO_2 adsorbed product. Therefore, this study will explore the basic strength distribution of the CaO/Fe_2O_3 and the carbonate morphology growth at different CO_2 adsorption times. In addition, infrared spectroscopy will be used to identify the formation of carbonate species and CO_2 adsorbed products on the bimetallic CaO/Fe_2O_3 surfaces.

MATERIALS AND METHODS

This work demonstrates the unique pattern of carbonate species and CO_2 product formations on the bimetallic metal oxide system. The synthesis details of CaO/Fe_2O_3 based on the most efficient adsorbent for CO_2 capture reported by Lahuri et al. (2017). Generally, 20 wt.% $Ca(NO_3)_2 \cdot 4H_2O$ from Fe_2O_3 was stirred in the mixture of distilled water and 25% (v/v) of ethanol. It was stirred for 2 h at room temperature and followed by ultrasonication for 30 min. The mixture was dried by stirring at 80-100 °C and the dried adsorbent was ground and calcined at 200 °C under ambient air for 2 h. The adsorbent was denoted as CaO/Fe_2O_3. The basicity strength distribution was measured using the chemisorption model Micromeritics 2920 Chemisorb.

The carbon monoxide-temperature programmed desorption (CO-TPD) analysis was performed to obtain the basic strength distribution of the bimetallic adsorbent. Approximately 50 mg were purged with He at 150 °C for 30 min to eliminate traces of moisture and humidity gases. For CO chemisorption, the pulse chemisorption method was applied by 20 times pulse of 5% CO in He (v/v) at 30 °C in which He flowed continuously as a carrier gas. The excess of CO and weak CO physisorption was desorbed at 50 °C under He gas flow for 30 min. The basicity strength distribution of CO adsorbed on the CaO/Fe_2O_3 surface was observed by performing TPD analysis from 30 to 900 °C at 10 °C/min. The effluent gas of desorbed CO was monitored quantitatively by a thermal conductivity detector.

A fluidized bed reactor was used to conduct CO_2 capture at various CO_2 adsorption times. Approximate 3 g of fresh CaO/Fe_2O_3 was cleaned by degassing with N_2 at 150 °C for 30 min to remove moisture content for better

and accurate adsorption. The temperature was cooled to room temperature for the CO_2 capture process. The 99% purity of CO_2 flowed at 30 mL/min at adsorption time of 4, 12, 24, and 36 h separately. The adsorbents were collected and characterized to observe the progress of carbonate formation at respective CO_2 adsorption times. The adsorbents were collected for further characterization by studying the pattern of carbonate formation on the adsorbent surfaces.

The fresh CaO/Fe_2O_3 was compared with CO_2 exposed at different adsorption times (4, 12, 24, and 36 h) using the following instruments. The morphology of the adsorbent was observed through micrograph images using field emission scanning electron microscope (FESEM) model LEO Supra 55VP which is equipped with energy dispersive X-ray (EDX). The EDX analysis was conducted to determine the element distribution on the adsorbent. Vibrational spectroscopy was used to study the presence of carbonate species and CO_2 adsorbed products on the adsorbent. Fourier transform infrared (FTIR) spectroscopy model GX, Perkin Elmer with the KBr pellet method for sample preparation was applied. The wavenumber was recorded in the range of 400 to 4000 cm^{-1}.

RESULTS AND DISCUSSION

Basicity strength is important to determine the affinity of the CaO/Fe_2O_3 adsorbent towards CO_2. The tendency of an acidic gas to be attracted to the surface basic site depending on the basicity strength of the adsorbent. The basic strength of the adsorbent was identified from the temperature region of the CO desorption. A stronger basicity strength possesses large bond energy which requires a higher temperature to desorb and vice versa. Thus, the strength of a particular CO chemisorbed can be identified by temperature interval wherein the basic site is desorbed. The basicity strength distribution was divided into weak, medium, strong and very strong regions at 40-250, 251-500, 501-700 and 701-900 °C, respectively (Hakim et al. 2016a).

The CO-TPD curve in Figure 1 shows that CaO/Fe_2O_3 exhibit an intense peak at the medium basic site with total basicity of 52.85 cm^3/g at a maximum desorption temperature of 453.8 °C. Hakim et al. (2016a) reported that Fe_2O_3 possesses total basicity from the adsorption quantity of 1.26 cm^3/g which is distributed at all basic sites of the weak, medium, strong, and very strong. Our previous work reported that CaO has a total basicity of 283.29 cm^3/g which was distributed at strong and very strong basic sites (Lahuri et al. 2017).

Besides, the desorption temperature ranges of 490-800 °C for CaO was agreed with Tang et al. (2019). It was noteworthy to observe the significant change in basicity strength of the CaO/Fe_2O_3 and its chemical shift of desorption temperature towards a lower range of 250-505 °C. CO molecule chemisorbs on transition metal oxide stronger than main groups metal oxide due to the chemical bonding on ions (Fe^{3+}) is stronger (Vesecky et al. 1994). It is because the Fe^{3+} possesses d orbital electrons which could overlap with CO 2 * antibonding orbitals (Chanapattharapol et al. 2017; Vesecky et al. 1994). Inversely, the chemical interaction between CO and CaO is expected to be weaker due to the absence of d electrons available for backbonding. Therefore, the chemical shift of the CO desorption temperature was observed due to the addition of CaO onto Fe_2O_3.

Naturally, increasing the basicity of the adsorbent by surface modification will enhance the CO_2 affinity. Based on the density functional calculations, CaO is highly active among alkaline earth metal oxides followed by MgO (Jensen et al. 2005; Pacchioni et al. 1994). It explains that an increasing lattice constant and decreasing Madelung potential led to the high reactivity of alkaline metal oxides. A low Madelung potential results in a more delocalized electron distribution of surface oxygen which overlaps with the orbitals of the adsorbing molecules. Besides, oxygen vacancy sites are highly catalytically active (Jensen et al. 2005) and highly efficient in charge transfer to adsorbates for metal oxides (Henderson et al. 1999). Thus, the presence of CaO enhances the basicity strength of Fe_2O_3 (Figure 1) which explains the reason adsorbent would have greater CO_2 affinity that is likely to form carbonate and higher efficiency in CO_2 capture.
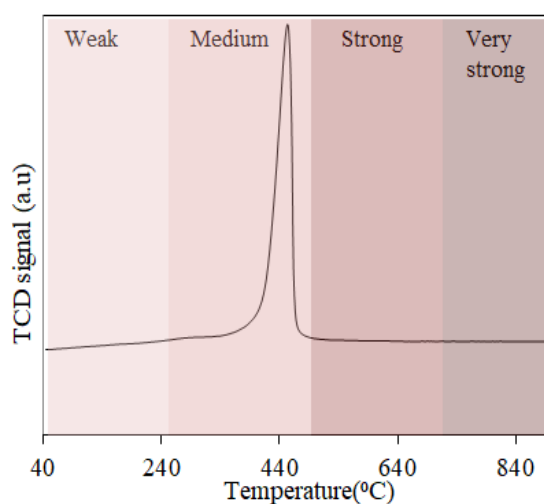

FIGURE 1. Basicity strength distribution by CO-TPD analysis

Morphology and the quantitative compositional element identification for the Fe_2O_3, fresh CaO/Fe_2O_3 and after various CO_2 adsorption times were analyzed using FESEM-EDX as shown in Figure 2. The morphology of the Fe_2O_3 alone describes a nano coral reef-like texture (Hakim et al. 2016a). In comparison with Fe_2O_3 alone, fresh CaO/Fe_2O_3 was observed to have an irregular sphere and ellipsoid particles with distinct sizes below 100 and above 200 nm. Therefore, it is confirmed that the larger size particles represent CaO, whereas the ultrasonication assisted method altered the original nano coral reef-like of Fe_2O_3 to irregular sphere and ellipsoid.

The carbonate growth on the CaO/Fe_2O_3 surfaces can be identified from the distinct fine particle at 36 h CO_2 adsorption compared to fresh CaO/Fe_2O_3. The trend of the carbonate growth was confirmed with the increment of the C element as the CO_2 adsorption contact time is longer.

Carbonate species and CO_2 adsorbed product formations on CaO/Fe_2O_3 were identified from the IR spectra described in Figure 3. The fresh Fe_2O_3 was observed to have the absorption bands that were associated with the inorganic interaction of Fe-O-Fe at 440, 475, 559, and 607 cm^{-1} (Hakim et al. 2016a). The addition of CaO on Fe_2O_3 increased the basicity site which
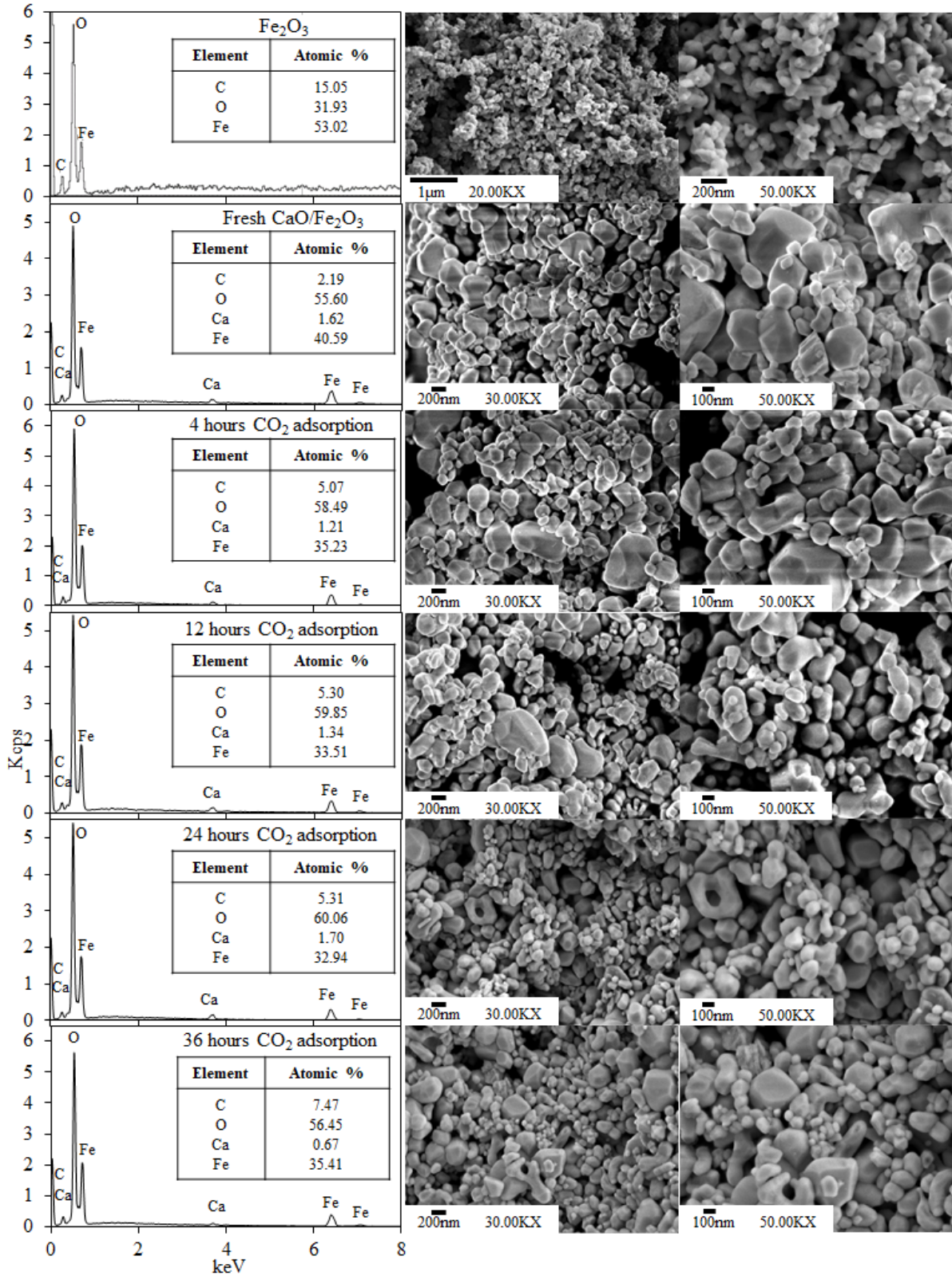
FIGURE 2. FESEM-EDX analysis of the fresh CaO/Fe$_2$O$_3$ and after CO$_2$ exposure
at 4, 12, 24 and 36 h

results in affinity to CO_2 from the environment. Thus, the absorption bands for fresh CaO/Fe_2O_3 at 1635 cm^{-1} was corresponded to the asymmetry O-C-O for bidentate carbonate, whereas 1046 and 1380 cm^{-1} were vibrational mode evidence of the C-O stretching and symmetry O-C-O, respectively, for monodentate carbonate. The assignment of the physisorbed CO_2 was detected at 2344 cm^{-1} (Hosakun 2017; Yang & Woll 2017). The sharp absorption at 825 cm^{-1} was attributed to adsorbed moisture and vibration of the OH groups on Fe_2O_3 agreed with Hassen Mohammed (2018). The absorption bands at 530 cm^{-1} (Hakim et al. 2016c) and 626 cm^{-1} (Kendix 2009) were also the signals for the inorganic interaction of Fe-O-Fe for Fe_2O_3. Meanwhile, a weak feature at 592 cm^{-1} was detected for the presence of longitudinal mode (vLO) of CaO (Hofmeister et al. 2003). The broad absorption around 3100-3700 cm^{-1} was assigned to the O-H stretch (Table 1).

After 4 h of CO_2 adsorption, the formation of carbonate species such as bicarbonate, monodentate carbonate and bidentate carbonate were prominent. Complete absorption bands for the carbonate species were detected. The presence of bicarbonate species was detected at 1428 and 1662 cm^{-1} which were attributed to symmetry O-C-O and asymmetry O-C-O, respectively (Baltrusaitis et al. 2011; Bargar et al. 2005; Di Cosimo et al. 1998; Ferretto & Glisenti 2002; Lefevre 2004; Su & Suarez 1997). The significant contribution to the presence of bicarbonate due to the O-H stretch at 3635 cm^{-1} (Hakim et al. 2016a). Another signal for monodentate carbonate was detected at 1576 cm^{-1} which corresponds to the assignment mode of asymmetry O-C-O (Baltrusaitis et al. 2011; Bargar et al. 2005; Di Cosimo et al. 1998; Ferretto & Glisenti 2002; Lefevre 2004; Su & Suarez 1997). The contribution of the band at 1250 cm^{-1} was assigned to the symmetry O-C-O for the bidentate carbonate (Baltrusaitis et al. 2011; Bargar et al. 2005; Ferretto & Glisenti 2002; Lefevre 2004). Formation of carbonate species by chemisorption, CO_3 (chem), occurred by CO_2 adsorption on oxygen sites of metal oxide (O_{sur-MO}) simplified in Equation 7. A quite variety of carbonate adsorption geometry is plausible (Burghaus 2014). Advanced techniques such as angle-resolved photoelectron spectroscopy (ARUPS), near edge X-ray absorption fine structure (NEXAFS) and photoelectron diffraction were used to determine the orientation of the carbonate (Davis et al. 1993).

$$CO_2 + O_{sur-MO} \ \square \ CO_3 \ chem \qquad (7)$$
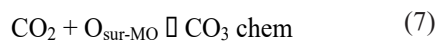
Meanwhile, nonlinear/bend CO_2 and bent charged $CO_2{}^{\gamma-}$ are commonly reported on reactive metal oxide surfaces such as MgO (Sawada et al. 1979) and CaO (Hlaing et al. 2016; Sun et al. 2016). Bent charged $CO_2{}^{\gamma-}$ can be considered a precursor to the formation of carbonate species (8).

$$CO_2 + O_{sur-MO} \ \square \ CO_2{}^{\gamma-} + O_{sur-MO} \ \square \ CO_3 \ (chem) \qquad (8)$$
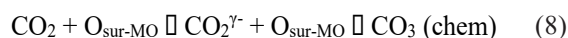
An increased contact time at 12 h of CO_2 adsorption, adsorbed carbonate results in inorganic interaction for $CaCO_3$ was detected at 544 cm^{-1} (Tlili et al. 2003). The assignment mode of bending CO_2 from the functional group of C=O was contributed to 668 cm^{-1} (Sun et al. 2016). Further CO_2 exposure at 24 h of contact time, another absorption band at 711 cm^{-1} was also ascribed to the $CaCO_3$. Since the CO_2 exposure was longer, the trace amount of moisture in the CO_2 gas tank leads to hydroxide compound formation as Fe-O-H deformation at 763 cm^{-1} (Bishop et al. 1997; Taylor 1980). This could be attributed to the presence of hydrogen bonded -C=O of carbonate groups at 1760 cm^{-1} (Zhang et al. 2013).

At this stage, the CO_2 adsorbed product on the CaO/Fe_2O_3 was expected to be saturated and it facilitates the multilayer CO_2 physisorption on the existing linear CO_2 which was identified at the absorption region of 2240-2402 cm^{-1} (Yang & Woll 2017). CO_2 physisorption on metal oxide as a CO_2 adsorbed product is simpler than carbonate formation. It does not involve electrons transfer but only weak interaction by forming linear CO_2 (Burghaus 2014). It was found that the interaction of CO_2 physisorption on metal oxide is stronger than that of metal surfaces based on the desorption temperature. The CO_2 adsorption on metal surfaces of metal oxide (M_{sur-MO}) leads to the CO_2 physisorption (phys) as shown in (9).

$$CO_2 + M_{sur-MO} \ \square \ CO_2 \ (phys) + M_{sur-MO} \qquad (9)$$
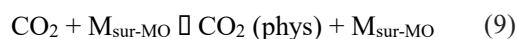
After 36 h of CO_2 adsorption, the contribution bands for the physisorption phenomenon of CO_2 adsorbed product in the form of linear CO_2 can be unambiguously identified at 2348, 2383, and 2394 cm^{-1} (Lv et al. 2015; Walker et al. 2004b). These bands were blueshifted from the isolated CO_2 at 2349 cm^{-1} (Walker et al. 2004b) which was assigned to the asymmetry stretch (v_3) linear CO_2, due to the different adjacent molecule interactions. The adsorption band at 2383 cm^{-1} can be associated with (one or two) CO_2 molecules bound directly to the metal ion (Gregoire et al. 2001; Walker et al. 2004a, 2004b; Xing et al. 2013). This peak has the feature described as core CO_2 because the interaction was formed around central coordination of metal ions that possesses higher binding energy. The vibration closest to the asymmetry

stretch (v_3) linear CO_2 at 2348 cm^{-1} was ascribed from the CO_2 bound to other CO_2 in the second layer region (Walker et al. 2004b). Meanwhile, the absorption band at 2394 cm^{-1} corresponds to one or more CO_2 attached to that rearranged cluster core since the strength of binding interaction is associated with blueshift (Walker et al. 2004a).
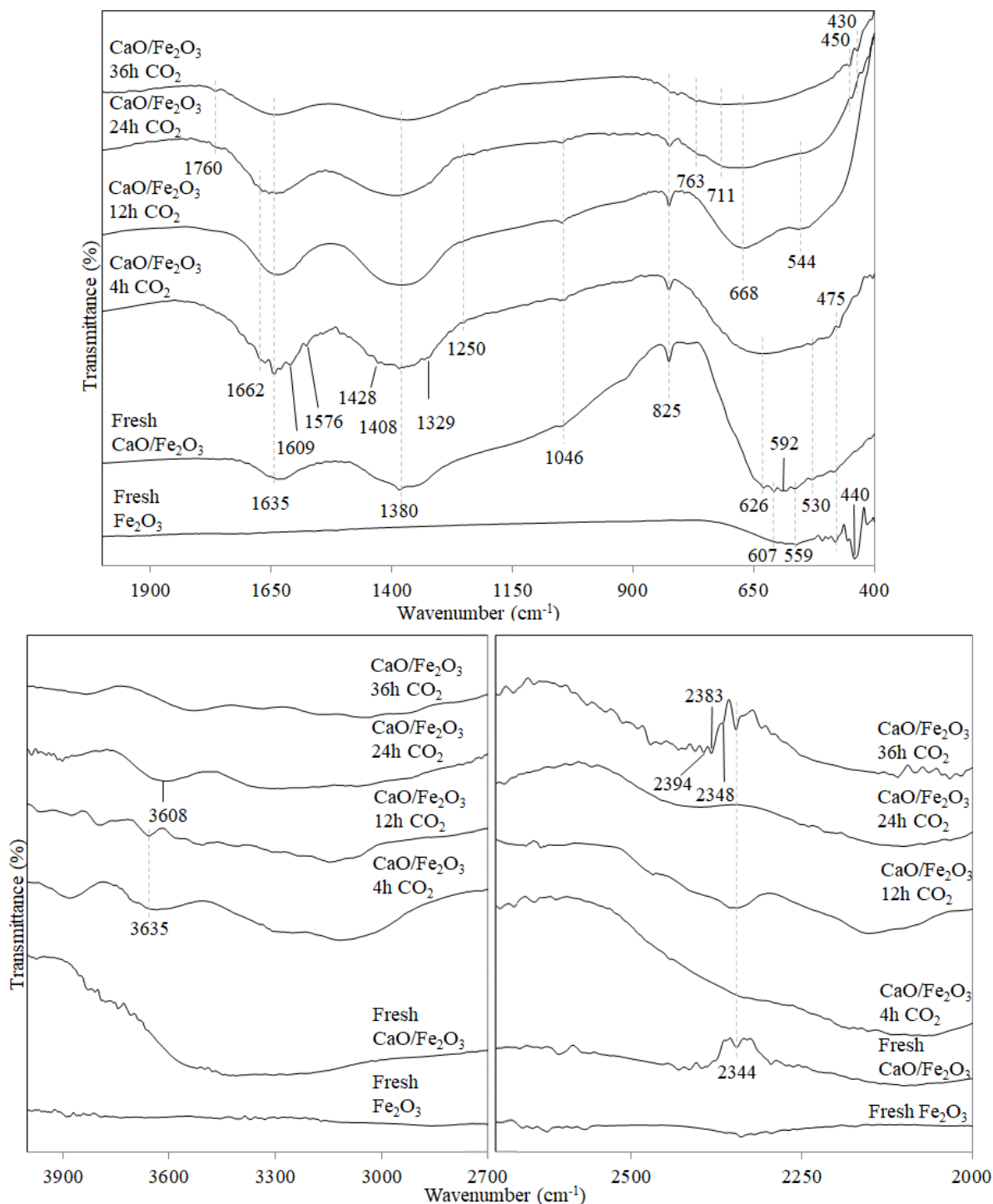

FIGURE 3. FTIR spectra for the CaO/Fe$_2$O$_3$ before and after CO_2 adsorption at a contact time of 4, 12, 24, and 36 h

TABLE 1. Vibrational frequencies for FTIR spectroscopy

Vibrational mode assignments	Experimental frequencies (cm^{-1})	Literature references (cm^{-1})
Fe-O-Fe for Fe_2O_3	440, 475, 530, 559, 607	440, 475, 530, 559, 607
$CaCO_3$	430, 450, 544, 626, 711	430, 480, 540, 623, 713
CaO	592	590
Bend CO_2 (C=O)	668	667
Fe-O-H	763, 825	775
Bicarbonate		
Symmetry O-C-O	1428	1396-1500
Asymmetry O-C-O	1662	1555-1720
O-H	3608, 3635	3600-3627
Monodentate carbonate		
C-O	1046	1046
Symmetry O-C-O	1380	1380-1395
Asymmetry O-C-O	1576	1446-1590
Bidentate carbonate		
Symmetry O-C-O	1250	1243-1355
Asymmetry O-C-O	1635	1530-1670
Hydrogen bonded -C=O of carbonate groups	1760	1760
Physisorption CO_2	2344	2240-2390
CO_2 bound to other CO_2	2348	2350
CO_2 bound to metal ion	2383	2375
CO_2 attached that rearranged cluster core	2394	2397-2402

Therefore, this study shows the bicarbonate species and linear CO_2 formation upon CO_2 capture onto the bimetallic system of CaO/Fe_2O_3, which is not reported by any researcher. The IR spectroscopy can be a useful tool to identify the formation of carbonate species and linear CO_2. Advance spectroscopy is suggested to explore the carbonate adsorption geometry onto the bimetallic system.

CONCLUSION

The addition of CaO onto Fe_2O_3 surfaces enhanced the surface basic site at a medium basic strength site with a maximum CO desorption temperature of 454 °C. The total basicity for the CO-TPD analysis was 52.85 cm^3g^{-1}, which was higher than Fe_2O_3 alone (1.26 cm^3g^{-1}).

CO_2 adsorption at 4, 12, 24, 36 h showed an increment of the C element through FESEM-EDX analysis with the carbonate formation in the form of fine aggregate particles was observed. Formation of carbonate species and linear CO_2 were identified on the bimetallic CaO/ Fe_2O_3 surfaces after CO_2 adsorption. Infrared spectra showed the presence of bicarbonate, monodentate carbonate and bidentate carbonate species after 4 h of CO_2 adsorption. CO_2 adsorbed product by physisorption was detected after 36 h of CO_2 adsorption at the region of 2240-2402 cm^{-1} in the form of linear CO_2. The absorption bands were assigned using isolated CO_2 of 2349 cm^{-1} as a guideline to other vibration signals due to its adjacent CO_2 interaction. It was found that linear CO_2 can be generated at the core layer where CO_2 is directly bound

to metal ions and the second layer due to the CO_2 bound to other CO_2.

REFERENCES

Abanades, J.C. 2002. The maximum capture efficiency of CO_2 using a carbonation/calcination cycle of $CaO/CaCO_3$. *Chemical Engineering Journal* 90(3): 303-306.

Abu Tahari, M.N., Lahuri, A.H., Ghazali, Z., Samidin, S., Sulhadi, S.S., Dzakaria, N. & Yarmo, M.A. 2020. Application of octadecylamine-based adsorbent on carbon dioxide capture. *Materials Science Forum* 1010: 367-372.

Abu Tahari, M.N., Hakim, A., Marliza, T.S., Mohd, N.H. & Yarmo, M.A. 2017a. XRD and CO_2 adsorption studies of modified silica gel with octadecylamine. *Materials Science Forum* 888: 529-533.

Abu Tahari, M.N., Hakim, A., Marliza, T.S. & Yarmo, M.A. 2017b. Carbon dioxide sorption by tetradecylamine supported on silica gel. *Malaysian Journal of Analytical Sciences* 21(4): 921-927.

Abu Tahari, M.N., Hakim, A., Tengku Azmi, T.S.M., Wan Isahak, W.N.R., Hisham, M.W.M. & Yarmo, M.A. 2016. Studies on adsorption-desorption of CO_2 by long chain fatty amine supported on SiO_2. *Materials Science Forum* 840: 343-347.

Abu Tahari, M.N., Hakim, A., Hisham, M.W.M. & Yarmo, M.A. 2015a. Modification of porous materials by saturated fatty amine as CO_2 capturer. *International Journal of Chemical Engineering and Applications* 6(6): 395-400.

Abu Tahari, M.N., Hakim, A., Wan Isahak, W.N.R., Samad, W.Z. & Yarmo, M.A. 2015b. Adsorption of CO_2 on octadecylamine-impregnated on SiO_2: Physical and chemical interaction studies. *Advanced Materials Research* 1087: 137-141.

Austin, N., Butina, B. & Mpourmpakis, G. 2016. CO_2 activation on bimetallic CuNi nanoparticles. *Progress in Natural Science: Materials International* 26(5): 487-492.

Bagherisereshki, E., Tran, J., Lei, F.Q. & AuYeung, N. 2018. Investigation into $SrO/SrCO_3$ for high temperature thermochemical energy storage. *Solar Energy* 160: 85-93.

Bakiz, B., Guinneton, F., Arab, M., Benlhachemi, A., Villain, S., Satre, P. & Gavarri, J.R. 2010. Carbonatation and decarbonatation kinetics in the La_2O_3-$La_2O_2CO_3$ system under CO_2 gas flows. *Advances in Materials Science and Engineering* 2010: 360597.

Baltrusaitis, J., Schuttlefield, J., Zeitler, E. & Grassian, V.H. 2011. Carbon dioxide adsorption on oxide nanoparticle surfaces. *Chemical Engineering Journal* 170(2-3): 471-481.

Bargar, J.R., Kubicki, J.D., Reitmeyer, R. & Davis, J.A. 2005. ATR-FTIR spectroscopic characterization of coexisting carbonate surface complexes on hematite. *Geochimica et Cosmochimica Acta* 69(6): 1527-1542.

Barker, R. 1973. The reversibility of the reaction $CaCO_3 \rightleftarrows CaO+CO_2$. *Journal of Applied Chemistry and Biotechnology* 23(10): 733-742.

Barker, S. & Ridgwell, A. 2012. Ocean acidification. *Nature Education Knowledge* 3(10): 21.

Bhagiyalakshmi, M., Lee, J.Y. & Jang, H.T. 2010. Synthesis of mesoporous magnesium oxide: Its application to CO_2 chemisorption. *International Journal of Greenhouse Gas Control* 4(1): 51-56.

Bishop, J.L., Murad, E., Madejova, J., Komadel, P., Wagner, U. & Scheinost, A.C. 1997 Visible, Mössbauer and infrared spectroscopy of dioctahedral smectites: Structural analyses of the Fe-bearing smectites sampor, SWy-1 and SWa-1. In *Proceedings of the 11th International Clay Conference*.

Bui, M., Adjiman, C.S., Bardow, A., Anthony, E.J., Boston, A., Brown, S., Fennell, P.S., Fuss, S., Galindo, A., Hackett, L.A. & Hallett, J.P. 2018. Carbon capture and storage (CCS): The way forward. *Energy & Environmental Science* 11(5): 1062-1176.

Burghaus, U. 2014. Surface chemistry of CO_2 - adsorption of carbon dioxide on clean surfaces at ultrahigh vacuum. *Progress in Surface Science* 89(2): 161-217.

Chanapattharapol, K.C., Krachuamram, S. & Youngme, S. 2017. Study of CO_2 adsorption on iron oxide doped MCM-41. *Microporous and Mesoporous Materials* 245: 8-15.

Davis, R., Walsh, J.F., Muryn, C.A., Thornton, G., Dhanak, V.R. & Prince, K.C. 1993. The orientation of formate and carbonate on ZnO(1010). *Surface Science* 298(1): L196-L202.

Di Cosimo, J.I., Diez, V.K., Xu, M., Iglesia, E. & Apesteguia, R. 1998. Structure and surface and catalytic properties of Mg-Al basic oxides. *Journal of Catalysis* 178(2): 499-510.

Ferretto, L. & Glisenti, A. 2002. Study of the surface acidity of an hematite powder. *Journal of Molecular Catalysis A: Chemical* 187(1): 119-128.

Galhotra, P. 2010. Carbon dioxide adsorption on nanomaterials. Carbon dioxide adsorption on nanomaterials. Dissertation, University of Iowa (Unpublished).

Gregoire, G., Velasquez, J. & Duncan, M.A. 2001. Infrared photodissociation spectroscopy of small Fe^+-$(CO_2)_n$ and Fe^+-$(CO_2)_n$Ar cluster. *Chemical Physics Letters* 349(5-6): 451-457.

Hakim, A., Marliza, T.S., Abu Tahari, M.N., Wan Isahak, W.N.R., Yusop, M.R., Hisham, M.W.M. & Yarmo, M.A. 2016a. Studies on CO_2 adsorption and desorption properties from various types of iron oxides (FeO, Fe_2O_3, and Fe_3O_4). *Industrial & Engineering Chemistry Research* 55(29): 7888-7897.

516

Hakim, A., Marliza, T.S., Abu Tahari, M.N., Yusop, M.R., Hisham, M.W.M. & Yarmo, M.A. 2016b. Development of α-Fe$_2$O$_3$ as adsorbent and its effect on CO$_2$ capture. *Materials Science Forum* 840(2016): 421-426.

Hakim, A., Yarmo, M.A., Marliza, T.S., Abu Tahari, M.N., Samad, W.Z., Yusop, M.R., Hisham, M.W.M. & Dzakaria, N. 2016c. The influence of calcination temperature on iron oxide (α-Fe$_2$O$_3$) towards CO$_2$ adsorption prepared by simple mixing method. *Malaysian Journal of Analytical Sciences* 20(6): 1286-1298.

Hakim, A., Abu Tahari, M.N., Marliza, T.S., Wan Isahak, W.N.R., Yusop, M.R., Hisham, M.W.M. & Yarmo, M.A. 2015a. Study of CO$_2$ adsorption and desorption on activated carbon supported iron oxide by temperature programmed desorption. *Jurnal Teknologi* 77(33): 75-84.

Hakim, A., Wan Isahak, W.N.R., Abu Tahari, M.N., Yusop, M.R., Hisham, M.W.M. & Yarmo, M.A. 2015b. Temperature programmed desorption of carbon dioxide for activated carbon supported nickel oxide: The adsorption and desorption studies. *Advanced Materials Research* 1087: 45-49.

Hare, A., Evans, W., Pocock, K., Weeke, C. & Gimenez, I. 2020. Contrasting marine carbonate systems in two fjords in British Columbia, Canada: Seawater buffering capacity and the response to anthropogenic CO$_2$ invasion. *PLoS ONE* 15(9): e0238432.

Hassen Mohammed, S.M. 2018. Characterization of magnetite and hematite using infrared spectroscopy. *Journal of Engineering Sciences & Information Technology* 2(1): 38-44.

Henderson, M.A., Epling, W.S., Perkins, C.L., Peden, C.H. & Diebold, U. 1999. Interaction of molecular oxygen with vacuum-annealed TiO$_2$ (110) surface: Molecular and dissociative channels. *Journal of Physical Chemistry B* 103(25): 5328-5337.

Heo, Y.J. & Park, S.J. 2017. Facile synthesis of MgO modified carbon adsorbents with microwave-assisted methods: Effect of MgO particles and porosities on CO$_2$ capture. *Scientific Reports* 7(1): 1-9.

Hlaing, N.N., Sreekantan, S., Hinode, H., Kurniawan, W., Thant, A.A., Othman, R., Mohamed, A.R. & Salime, C. 2016. Effect of carbonation temperature on CO$_2$ adsorption capacity of CaO derived from micro/nanostructured aragonite CaCO$_3$. *AIP Conference Proceedings* 1733(1): 020023.

Ho, T.H., Howes, T. & Bhandari, B.R. 2014. Encapsulation of gases in powder solid matrices and their applications: A review. *Powder Technology* 259: 87-108.

Hofmeister, A.M., Keppel, E. & Speck, A.K. 2003. Absorption and reflection infrared spectra of MgO and other diatomic compounds. *Monthly Notices Royal Astronomy Society* 345(1): 16-38.

Horiuchi, T., Hidaka, H., Fukui, T., Kubo, Y., Horioa, M., Suzukia, K. & Mori, T. 1998. Effect of added basic metal oxides on CO$_2$ adsorption on alumina at elevated temperatures. *Applied Catalysis A: General* 167(2): 195-202.

Hosakun, Y., Halász, K., Horváth, M., Csóka, L. & Djoković, V. 2017. ATR-FTIR study of the interaction of CO$_2$ with bacterial cellulose-based membranes. *Chemical Engineering Journal* 324: 83-92.

Ismail, H.M., Cadenhead, D.A. & Zaki, M.I. 1997. Surface reactivity of iron oxide pigmentary powders toward atmospheric components: XPS, FESEM, and gravimetry of CO and CO$_2$ adsorption. *Journal of Colloid and Interface Science* 194(2): 482-488.

Jensen, M.B., Pettersson, L.G.M., Swang, O. & Olsbye, U. 2005. CO$_2$ sorption on MgO and CaO surfaces: A comparative quantum chemical cluster study. *Journal of Physical Chemistry B* 109(35): 16774-16781.

Kendix, E.L. 2009. Transmission and reflection (ATR) far-infrared spectroscopy applied in the analysis of cultural heritage materials. Thesis. Universita di Bologna (Unpublished).

Kumar, S., Saxena, S.K., Drozd, V. & Durygin, A. 2015. An experimental investigation of mesoporous MgO as a potential pre-combustion CO$_2$ sorbent. *Materials for Renewable and Sustainable Energy* 4(2): 1-8.

Lahuri, A.H., Adnan, R., Mansor, M.H., Waheed Tajudeen, N.F. & Nordin, N. 2020a. Adsorption kinetics for carbon dioxide capture using bismuth(III) oxide impregnated on activated carbon. *Malaysian Journal of Chemistry* 22(1): 33-46.

Lahuri, A.H., Michael Ling, N.K., Abdul Rahim, A. & Nordin, N. 2020b. Adsorption kinetics for CO$_2$ capture using cerium oxide impregnated on activated carbon. *Acta Chimica Slovenica* 67(2): 570-580.

Lahuri, A.H., Yarmo, M.A., Abu Tahari, M.N., Marliza, T.S., Tengku Saharuddin, T.S., Mark Lee, W.F. & Dzakaria, N. 2020c. Comparative adsorption isotherm for beryllium oxide/iron (III) oxide toward CO$_2$ adsorption and desorption studies. *Materials Science Forum* 1010: 361-366.

Lahuri, A.H., Yarmo, M.A., Marliza, T.S., Abu Tahari, M.N., Samad, W.Z., Dzakaria, N. & Yusop, M.R. 2017. Carbon dioxide adsorption and desorption study using bimetallic calcium oxide impregnated on iron(III) oxide. *Materials Science Forum* 888: 479-484.

Lefevre, G. 2004. *In situ* Fourier-transform infrared spectroscopy studies of inorganic ions adsorption on metal oxides and hydroxides. *Advances in Colloid and Interface Science* 107(2-3): 109-123.

Luis, P. 2016. Use of monoethanolamine (MEA) for CO$_2$ capture in a global scenario: Consequences and alternatives. *Desalination* 380: 93-99.

Lv, P., Almerida, G. & Perre, P. 2015. TGA-FTIR analysis of torrefaction of lignocellulosic components (cellulose, xylan, lignin) in isothermal conditions over a wide range of time durations. *BioResources* 10(3): 4239-4251.

Manovic, V., Wu, Y.H., He, I. & Anthony, E.J. 2011. Core-in-shell CaO/CuO-based composite for CO$_2$ capture. *Industrial & Engineering Chemistry Research* 50(22): 12384-12391.

Naeem, M.A., Armutlulu, A., Imtiaz, Q. & Muller, C.R. 2017. CaO-based CO$_2$ sorbents effectively stabilized by metal oxides. *ChemPhysChem* 18(22): 3280-3285.

Okawa, Y. & Tanaka, K. 1995. STM investigation of the reaction of Ag-O added rows with CO_2 on a Ag(110) surface. *Surface Science* 344(3): L1207-L1212.

Pacchioni, G., Ricart, J.M. & Illas, F. 1994. *Ab initio* cluster model calculations on the chemisorption of CO_2 and SO_2 probe molecules on MgO and CaO(100) surfaces. A theoretical measure of oxide basicity. *Journal of American Chemical Society* 116(22): 10152-10158.

Roger, B.R. & Girdler Corp. 1930. Process for separating acidic gases. U.S. Patent 1,783,901.

Rosynek, M.P. & Magnuson, D.T. 1977. Infrared study of carbon dioxide adsorption on lanthanum sesquioxide and trihydroxide. *Journal of Catalysis* 48(1-3): 417-421.

Salvador, C., Lu, D., Anthony, E.J. & Abanades, J.C. 2003. Enhancement of CaO for CO_2 capture in an FBC environment. *Chemical Engineering Journal* 96(1-3): 187-195.

Sawada, Y., Yamaguchi, J., Sakurai, O., Uematsu, K., Mizutani, N. & Kato, M. 1979. Thermal decomposition of basic magnesium carbonates under high-pressure gas atmoshpheres. *Thermochimica Acta* 32(1-2): 277-291.

Silaban, A. & Harrison, D.P. 1995. High temperature capture of carbon dioxide: Characteristics of the reversible reaction between CaO(s) and CO_2(g). *Chemical Engineering Communications* 137(1): 177-190.

Slostowski, C., Marre, S., Dagault, P., Babotb, O., Toupanceb, T. & Aymonier, C. 2017. CeO_2 nanopowders as solid sorbents for efficient CO_2 capture/release processes. *Journal of CO₂ Utilization* 20: 52-58.

Su, C.M. & Suarez, D.L. 1997. *In situ* infrared speciation of adsorbed carbonate on aluminium and iron oxides. *Clays and Clay Minerals* 45(6): 814-825.

Sun, Z., Wang, J., Du, W., Lu, G., Li, P., Song, X. & Yu, J. 2016. Density functional theory study on the thermodynamics and mechanism of carbon dioxide capture by CaO and CaO regeneration. *RSC Advances* 6(45): 39460-39468.

Takahashi, H., Yuki, K. & Nitta, T. 2002. Chemical modification of rutile TiO_2(1 1 0) surface by *ab initio* calculations for the purpose of CO_2 adsorption. *Fluid Phase Equilibria* 194: 153-160.

Tang, Y., Liu, H., Ren, H.M., Cheng, Q.T., Cui, Y. & Zhang, J. 2019. Development KCl/CaO as a catalyst for biodiesel production by tri-component coupling transesterification. *Environmental Progress & Sustainable Energy* 38(2): 647-653.

Taylor, R.M. 1980. Formation and properties of Fe (II) Fe (III) hydroxyl-carbonate and its possible significance in soil formation. *Clay Minerals* 15(4): 369-382.

Tlili, M.M., Ben Amor, M., Gabrielli, C., Joiret, S., Maurin, G. & Rousseau, P. 2003. Study of electrochemical deposition of $CaCO_3$ by *in situ* raman spectroscopy. *Journal of the Electrochemical Society* 150(7): C485-C493.

Vesecky, S.M., Xu, X.P. & Goodman, D.W. 1994. Infrared study of CO on NiO(100). *Journal of Vacuum Science & Technology A* 12(4): 2114-2118.

Walker, N.R., Walters, R.S. & Duncan, M.A. 2004a. Infrared photodissociation spectroscopy of $V^+(CO_2)_n$ and $V^+(CO_2)_n$Ar complexes. *Journal of Chemical Physics* 120(21): 10037-10045.

Walker, N.R., Walters, R.S., Grieves, G.A. & Duncan, M.A. 2004b. Growth dynamics and intracluster reactions in $Ni^+(CO_2)_n$ complexes via infrared spectroscopy. *Journal of Chemical Physics* 121(21): 10498-10507.

Wan Isahak, W.N.R., Che Ramli, Z.A., Lahuri, A.H., Yusop, M.R., Hisham, M.W.M. & Yarmo, M.A. 2015. Enhancement of CO_2 capture using CuO nanoparticles supported on green activated carbon. *Advanced Materials Research* 1087: 111-115.

Wang, Y.M., Kovacik, R., Meyer, B., Kotsis, K., Stodt, D., Staemmler, V., Qiu, H.S., Traeger, F., Langenberg, D., Muhler, M. & Woll, C. 2007. CO_2 activation by ZnO through the formation of an unusual tridentate surface carbonate. *Angewandte Chemie International Edition* 46(29): 5624-5627.

Whateley, T.L. 1971. Carbonate species and not polywater formed on magnesium oxide. *Nature Physical Science* 231(25): 178-179.

Xing, X.P., Wang, G.J., Wang, C.X. & Zhou, M.F. 2013. Infrared photodissociation spectroscopy of $Ti^+(CO_2)_2$Ar and $Ti^+(CO_2)_n$ (n=3-7) complexes. *Chinese Journal of Chemical Physics* 26(6): 687-693.

Yang, C.W. & Woll, C. 2017. IR spectroscopy applied to metal oxide surfaces: Adsorbate vibrations and beyond. *Advances in Physics* X2(2): 373-408.

Yoshikawa, K., Sato, H., Kaneeda, M. & Kondo, J.N. 2014. Synthesis and analysis of CO_2 adsorbents based on cerium oxide. *Journal of CO₂ Utilization* 8: 34-38.

Yuan, Z.H. & Eden, M.R. 2016. Toward the development and deployment of large-scale carbon dioxide capture and conversion processes. *Industrial & Engineering Chemistry Research* 55(12): 3383-3419.

Zhang, Z.P., Rong, M.Z., Zhang, M.Q. & Yuan, C. 2013. Alkoxyamine with reduced homolysis temperature and its application in repeated autonomous self-healing of stiff polymer. *Polymer Chemistry* 4(17): 4648-4654.

Azizul Hakim Lahuri*
Department of Science and Technology
Universiti Putra Malaysia Bintulu Kampus
P.O Box 396, Nyabau Road
97008 Bintulu, Sarawak
Malaysia

Mohd Ambar Yarmo
Department of Chemical Sciences
Faculty of Science and Technology
Universiti Kebangsaan Malaysia
43600 UKM Bangi, Selangor Darul Ehsan
Malaysia

*Corresponding author; email: azizulhakim@upm.edu.my